CORE
Metadata, citation and similar papers at core.ac.uk
Provided by Helsingin yliopiston digitaalinen arkisto

BOREAL ENVIRONMENT RESEARCH 12: 409–420
Helsinki 25 June 2007
ISSN 1239-6095
© 2007

Chemical composition of waterfall-induced air ions: spectrometry *vs.* simulations

Tiia-Ene Parts[1)], Aare Luts[1)], Lauri Laakso[2)], Anne Hirsikko[2)], Tiia Grönholm[2)] and Markku Kulmala[2)]

[1)] *Institute of Environmental Physics, University of Tartu, Ülikooli 18, 50090 Tartu, Estonia*
[2)] *Department of Physical Sciences, P.O. Box 64, FI-00014 University of Helsinki, Finland*

Received 8 Nov. 2006, accepted 30 Apr. 2007 (Editor in charge of this article: Veli-Matti Kerminen)

Parts, T.-E., Luts, A., Laakso, L., Hirsikko, A., Grönholm, T. & Kulmala, M. 2007: Chemical composition of waterfall-induced air ions: spectrometry *vs.* simulations. *Boreal Env. Res.* 12: 409–420.

Our measurements of ion size distributions near a waterfall provided new evidence for a waterfall-induced modification of air ion sizes. The ion size spectrum near a waterfall permanently differs from that in ordinary tropospheric air. In this paper we investigated the near-waterfall air ions chemical nature in detail. We carried out a simulation series of air small negative ion evolution, proposing that falling water, as a new environmental component, increases the concentration of OH^- cluster ions. The produced OH^- ions were employed as an extra input for our ion evolution model. The presence of additional OH^- ions resulted in a decrease of typically model-provided NO_3^- and/or HSO_4^- cluster ion concentrations and an increase of the abundance of HCO_3^- cluster ions. Near the waterfall the latter ions became dominant in our simulations.

Introduction

Already in 1892, Philipp Lenard published the first comprehensive paper about the electricity of waterfalls. He established that natural falling water produces negatively-charged particles. Although that long period of time elapsed since the publication of Lenard's paper, it remains unsolved what kind of negative-charged particles are responsible for this effect. Only certain details of this and the related effects were elucidated.

Starting from the studies by Blanchard, the main attention was paid to the charge arising from near the sea surface. This "Blanchard effect" was supposed to be partly responsible for the atmospheric electric field. Recent studies showed that the outcome of this effect depends on several factors and that under certain conditions the "classical" effect does not hold. However, the researchers carried out many experiments and demonstrated several peculiarities (Blanchard 1958, Gathman and Trent 1968, Reiter 1994, Klusek *et al*. 2004). Much attention was paid also to the mechanism of electrospray ionisation (ESI). The problem crucial for the ESI is how spray droplets produce ions. ESI conditions are rather different from those that characterize natural waterfalls (different electric fields, different chemical contents of the droplets, etc.). Despite intensive studies, the ESI mechanism has not been completely unravelled (Kebarle and Peschke 2000, Cech and Enke 2001).

The classical "waterfall effect" is even less understood than the ESI mechanism. Chapman (1937) obtained some waterfall-like spray parti-

cle mobility spectra in laboratory measurements and studied how the spectra depend on chemical impurities in water. Reiter (1994) measured particle size spectra near a natural waterfall, but these spectra contained only four measurement points. No definite mechanism of the waterfall effect has been proposed. The specific changes in ion size spectra caused by natural waterfalls have remained unknown until very recently (Laakso *et al*. 2006).

Earlier studies revealed chemical mechanisms that can be attributed to the waterfall effect (Iribarne and Thomson 1976, Znamenskiy *et al*. 2003, Vostrikov *et al*. 2006). Several researchers have studied the molecular properties of water. Because of the versatility of hydrogen bonds, water can form shells even around complex molecules. In addition, the "magic" complexes of water molecules are known (Finney 2004, Shin *et al*. 2004, Zwier 2004). These complexes are far more stable than other complexes.

The evolution of air ions has commonly been considered the evolution of ion nature (transformations of ion cores). There is some evidence that the size and mobility of cluster ions depend more on the number of water molecules in the cluster than on other chemical fragments within it (Han *et al*. 2003). As a result, water chemistry can drive the formation channels of airborne particles more effectively than what has been previously thought. Weakly-bound water clusters raised substantial interest (Ludwig 2001, Finney 2004). Despite their low concentrations, complexes between water and other atmospheric species can play an important role in the chemistry of the atmosphere (Sennikov *et al*. 2005).

It is known that liquid water (e.g., in droplets) contains OH^- and H^+ ions due to the autoionisation and that these ions determine the pH of water solutions (Brown *et al*. 2006). Thus, under certain circumstances, liquid water can be a source of OH^- ions. Recent mass spectrometric measurements revealed that at higher concentrations of water in purified air, the relative abundance of OH^- clusters increases (Nagato *et al*. 2006). The OH^- ions are important to understanding the waterfall effect. A model on how a waterfall can produce extra OH^- ions was proposed by Laakso *et al*. (2006). It should be mentioned that traditional atmospheric chemistry deals mainly with OH radicals, not with OH^- ions. Tropospheric hydroxyl radicals arise due to a sum of photochemical reactions, but these processes generate no hydroxyl ions (Seinfeld and Pandis 1998, Sennikov *et al*. 2005). Tropospheric OH^- ions can be produced by ionising radiation. Already Huertas *et al*. (1978) treated the effect of OH^- upon the evolution of small negative ions. Huertas *et al*. (1978) introduced a pioneering, yet tentative model, and did not set OH^- ions into the context of waterfall.

The results of our measurements, performed at a waterfall in Helsinki, Finland, demonstrated that air ion spectra differed distinctively from the reference spectra (Laakso *et al*. 2006). In this paper we will investigate the chemical nature of new air ions in more detail. We will briefly describe our previous measurements and simulation model, after which we will consider observations and derive some quantities needed for correct initialisation of our simulation model. Finally we will discuss the simulation outcomes and conclude our results.

Methods and general constraints

Description of the measurement conditions

In our previous study we reported measured ion size distributions near waterfalls and suggested possible pathways leading to these distributions (Laakso *et al*. 2006). The measurements were made in Vantaanputous, a waterfall approximately five kilometres northeast of the city centre of Helsinki, Finland. We used two air ion spectrometers in the measurements: one on a bridge approximately 20 meters from the edge of the waterfall and the other (as a reference) about 100 meters from the waterfall.

The air ion spectrometer (manufactured by AIREL Ltd., Estonia) measures the mobility/size distributions of positive and negative air ions in a mobility range of 3.16–0.00133 $cm^2\ V^{-1}\ s^{-1}$, with a corresponding diameter range being 0.34–40.3 nm. The diameters were calculated with the algorithm derived by Tammet (1995) for the temperature of 273 K and pressure of 1013 hPa. For further information about the ion spectrom-

eter, the reader may consult papers by Laakso *et al*. (2006) and Mirme *et al*. (2007), as well as http://www.airel.ee. This spectrometer is an advanced instrument that enabled us to obtain the first detailed ion spectra near waterfall.

Description of the simulation model

We simulated the negative air ion evolution with a mathematical model that is essentially the same as the one discussed by Luts and Parts (2002). Recently, Luts *et al*. (2004) complemented this model with new data about ion-molecule reactions involving sulphuric acid. The new model version contains quite heavy negative species such as $HSO_4^-\bullet(H_2SO_4)_6\bullet(H_2O)_{18}$. The description of the model, especially its mathematical characteristics, was presented by Luts (1998). In the following we outline a brief summary of the model.

The model is limited to small ions, the evolution of which is simulated by a system of differential equations given by

$$d\boldsymbol{Y}/dt = \mathbf{A}\boldsymbol{Y} - \mathbf{B}\boldsymbol{Y} + \boldsymbol{Q}. \qquad (1)$$

Here t is the time, $\boldsymbol{Y} = \boldsymbol{Y}(t)$ is the vector of ion concentrations, $\mathbf{A}$ is the matrix describing the rates of ion-molecule reactions, $\mathbf{B}$ is the matrix presenting the decay (recombination) of ions, and $\boldsymbol{Q}$ is the ion generation rate vector. The evolution model yields the time variation of the ion concentration vector $\boldsymbol{Y} = \boldsymbol{Y}(t)$. With additional tools, we can also obtain, for example, the steady state composition of ions.

If compared with the ion evolution model by Huertas *et al*. (1978), our model contains much more ion species, much more neutral species and much more routes for the evolution of ions. The model takes into account 166 ion species, 127 neutral species and 522 ion-molecule reactions. During a simulation, concentrations of neutral species are assumed to be in a steady state, i.e. constant during the period of interest. Therefore, all background effects such as the uptake of sulphuric acid by aerosol particles and reactions between neutral species are already included in these "steady-state" concentrations. This constraint can add some inaccuracy but it is quite a common practice in these kind of models and can be justified as well. As a rule, concentrations of neutral species are very large (typically more than several million cm^{-3}) as compared with concentrations of small ions (typically a few hundred cm^{-3}). Ion-molecule reactions alone can hardly modify the steady-state concentrations of neutral species, especially considering a local situation (such as near a waterfall). The only choise for these modifications is to proceed very slowly because of the large concentrations of neutral species. Additionally, steady-state local concentrations of neutral species are continuously supported by the other processes. Therefore, although our constraint can cause some small inaccuracies, it will significantly simplify the mathematical treatment of processes in the model.

We consider ions "small" as long as their evolution can be successfully described by means of a set of ion-molecule reactions. Small ions have mobilities down to about 0.5 $cm^2\ V^{-1}\ s^{-1}$ and diameters of less than 1.5 nm (Tammet 1995). In natural air, small (cluster) ion concentrations range from a few hundreds to one thousand ions cm^{-3} (e.g. Hirsikko *et al*. 2005). The basic ion transformation processes used in our model can be described using a scheme (Fig. 1). The main routes for the evolution of ions are marked by continuous lines, whereas less important routes are marked by dashed lines. The term "route" denotes direct or mediated (through not implicitly-included ions) transformation process. The formulae surrounded by frames indicate ion classes, except the frame with "X..." in it which denotes "something else". By "something else" we mean all the ions that are far less abundant than the marked ions. We specify the term "ion class" later (*see* section "Simulation results"). The symbols X and Y stand for chemical fragments that may join with ion cores in the course of clustering. Typical such fragments are H_2O, HNO_3 and H_2SO_4.

Commonly, the evolution of negative air ions starts with a mixture of primary O_2^- and O^- ions. In this case the main steady-state small clusters are the ion classes $NO_3^-\bullet X\bullet Y$ and $HSO_4^-\bullet X\bullet Y$. Near a waterfall, an additional source of (primary) ions appears. Laakso *et al*. (2006) discussed potential pathways leading to the formation of new ions. For example, small fragments

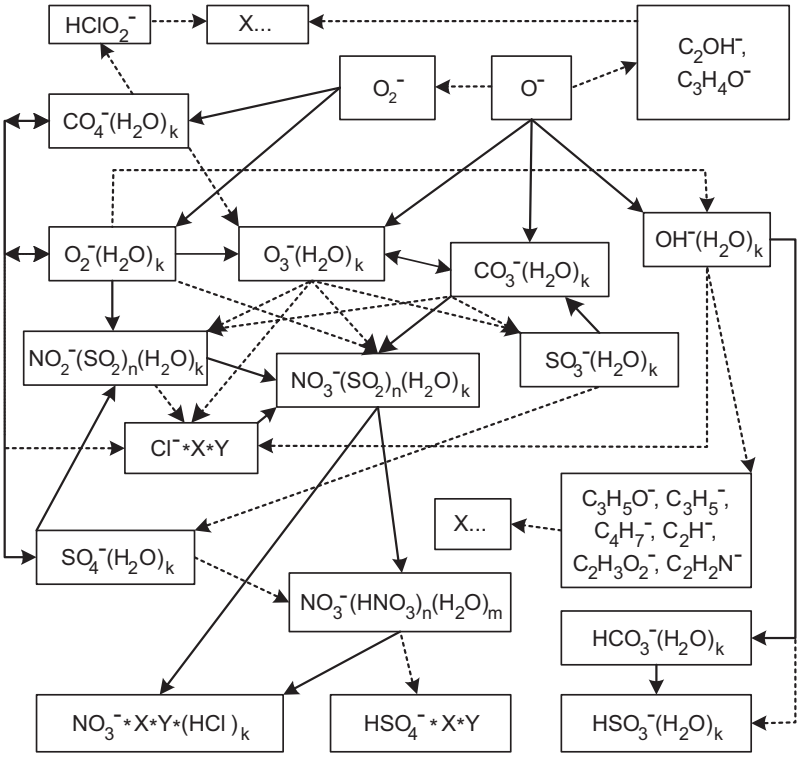

Fig. 1. The basic scheme of the negative ion transformation processes. For details, *see* section "Description of the simulation model".

torn away from the surfaces of water droplets bear a negative charge, whereas the remaining droplet becomes positively charged:

$$(H_2O)_n \longrightarrow H_3O^+(H_2O)_{n-m} + OH^-(H_2O)_{m-2}, \quad (2)$$

where $m << n$. Far away from a waterfall, this additional source of OH^- ions disappears. Thus, in most cases ion evolution models can neglect the OH^- ions.

The aim of our simulations was to investigate situations in which an additional source of OH^- ions exists. We included a number of various background situations. In all the cases, we searched for a specific steady-state ion composition that can be attributed to the natural spectrum. This means that we were looking for the composition that will remain constant until the background situation will change. The background situation can be characterized by several factors, including the background aerosol concentration, ion production rate and concentrations of neutral compounds. In order to obtain the steady-state composition, we averaged the computed ion concentration vector $\boldsymbol{Y} = \boldsymbol{Y}(t)$ over the lifetime of ions by taking into account all relevant factors. The mean lifetime of natural air ions is up to several hundred seconds. This procedure gives a composition that is close to the natural concentration (Luts 1998).

Results and discussion

Observed ions near the waterfall

According to our measurements, the waterfall steadily modified air ion spectra near the waterfall in comparison with spectra in the reference point (Figs. 2–4). In case of negative ions, we observed a moderate increase in small ion concentrations, a multi-fold increase in intermediate ion concentrations, and a minor to moderate increase in large ion concentrations. In case of positive ions, we observed a minor decrease in concentrations of small ions, a moderate increase in concentrations of intermediate ions, and a minor increase in concentrations of large ions.

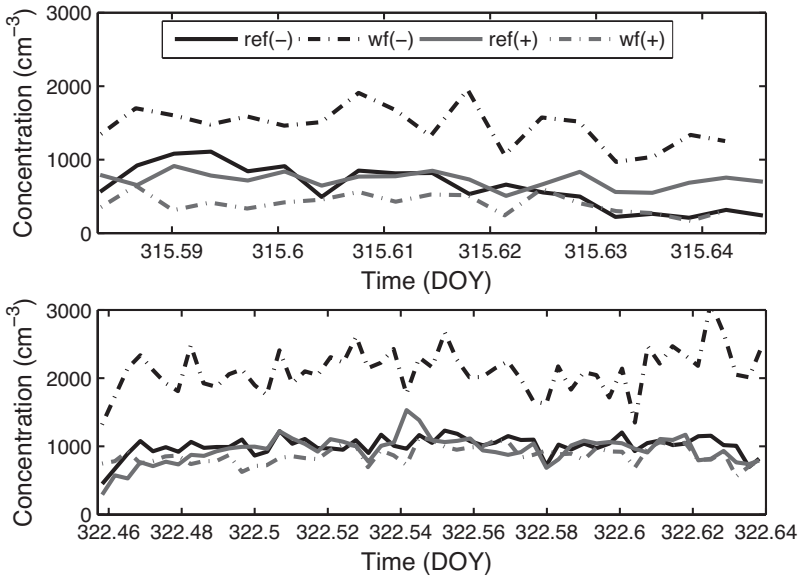

Fig. 2. Temporal variations of cluster (< 1.5 nm) ions near the waterfall and at the reference point on 11 (top) and 18 (bottom) November 2005. For details and discussion, *see* sections "Description of the measurement conditions" and "Observed ions near waterfall", and Laakso *et al.* (2006).

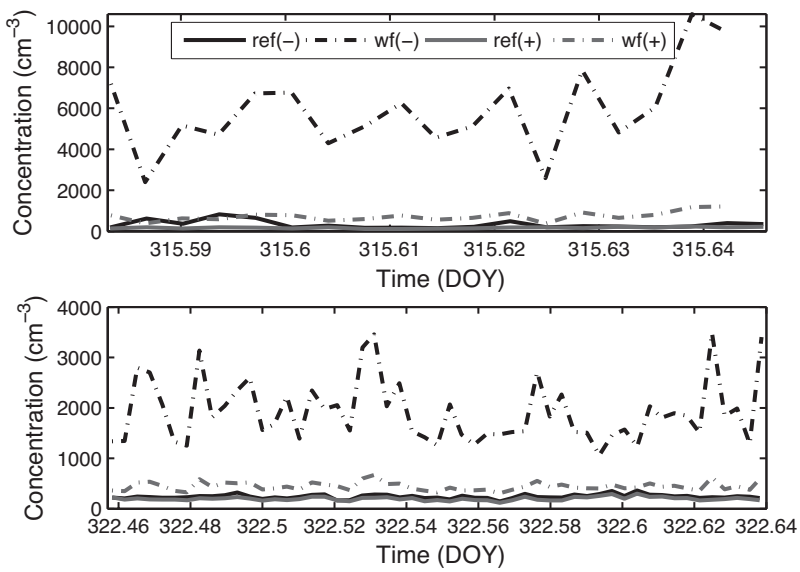

Fig. 3. Temporal variations of intermediate (1.5–10 nm) ions. For other information, *see* the caption of Fig. 2.

The minor decrease in the concentration of small positive ions is reasonable. Since the waterfall produced a large number of particles of all sizes, small ions can readily attach to background particles. This would apply also to small negative ions in the absence of an additional source for them. However, small negative ions were more abundant near the waterfall (Fig. 2), so the waterfall appears to have produced these ions. The production rate of these ions can be derived from the ion balance equation, provided that all the necessary parameters are known (Tammet and Kulmala 2005). Unfortunately, the whole effective aerosol spectrum was not measured. We estimated the production rate of small negative ions by estimating the total background aerosol concentration far from the waterfall and by taking into account changes in measured ion spectra when moving from near the waterfall to far from it (Figs. 2–4).

The average concentration of small ions measured far from the waterfall was about 1000 cm^{-3} (Fig. 2). Let us assume that the small ion production rate far from waterfall was 5 cm^{-3} s^{-1}

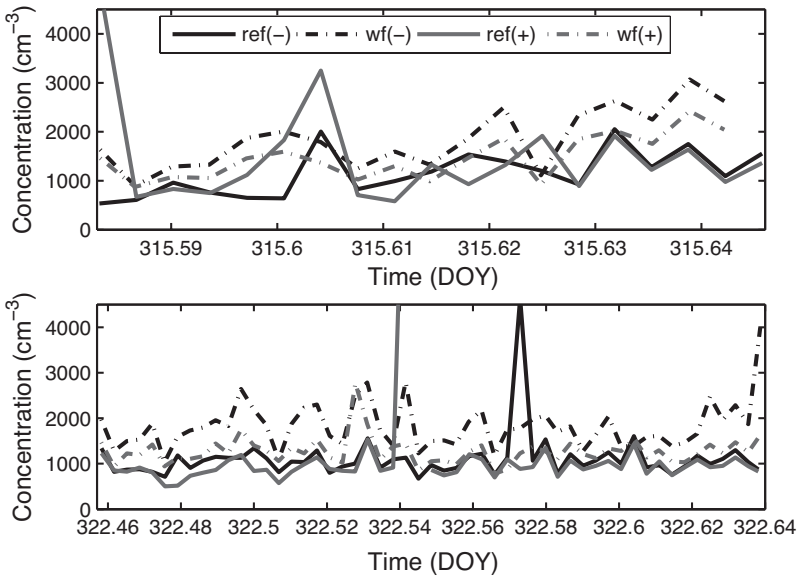

Fig. 4. Temporal variations of large (10–40 nm) ions. For other information, *see* the caption of Fig. 2.

(e.g. Laakso *et al*. 2004). The attachment rate of small ions onto aerosol particles depends not only on the concentration of aerosol particles but also on the shape of the aerosol spectrum (Tammet and Kulmala 2005). The average effective value of this attachment coefficient has been calculated to be 1.3×10^{-6} cm^3 s^{-1} (Salm 1987). In order to obtain the measured average value of small ions (1000 cm^{-3}; Fig. 2), the total aerosol concentration should have been about 2600 cm^{-3}. The measured concentration of intermediate ions was about a few hundred cm^{-3}, so let us choose a value of 300 cm^{-3} (Fig. 3). The measured concentration of large ions varied usually in the range 1000–3000 cm^{-3}, so let us choose a value of 1500 cm^{-3} (Fig. 4). When comparing the sum of these values (300 + 1500 cm^{-3}) to that obtained from the ion balance equation (2600 cm^{-3}), we deduce that there were 800 particles cm^{-3} in that part of the particle size spectrum that was outside of our measurement range. The estimated value does not contradict with the measured one.

Now, let us consider the situation near the waterfall. The measured average concentration of small positive ions was about 500 cm^{-3} and that of small negative ions was about 2000 cm^{-3} (Fig. 2). For positive ions, we assumed the ion production rate to be equal to 5 cm^{-3} s^{-1} and employed the ion balance equation again. In order to obtain the measured concentration of positive ions, the total aerosol concentration should have been about 7000 cm^{-3}.

Concentration of large ions were not considerably different between the waterfall and reference point (Fig. 4), whereas concentrations of intermediate negative ions increased on average by about 4000 cm^{-3} near the waterfall (Fig. 3). Therefore, this new total aerosol concentration 7000 cm^{-3} seems acceptable (the previous concentration of 2600 cm^{-3} + the increase of 4000 cm^{-3} + 400 particles cm^{-3} that are in that part of the size spectrum that is outside of our measurement range).

By using the aerosol concentration of 7000 cm^{-3}, we next try to calculate the production rate of small negative ions. In order to obtain a new data set for the ion balance equation, we take into account the fact that negative small ions do not attach to negative intermediate ions (Tammet and Kulmala 2005). Therefore, for the ion balance equation, the estimated total aerosol concentration (7000 cm^{-3}) should be reduced by the extra amount of negative intermediate ions (4000 cm^{-3}). Thus, we end up with a total aerosol concentration of 3000 cm^{-3}. In this case, the ion balance equation yields a production rate of 17 cm^{-3} s^{-1} for negative ions.

The waterfall appears to produce at least ten additional small negative ions per cubic centimetre per second. While this value was derived from

measured data, we did not take into account temporal variations that were sometimes rather large (Figs. 2–4). Nevertheless, within these constraints the result is consistent with the measured values and also demonstrates that waterfall can produce even more small ions than what the ionising radiation does. The produced new ions will be served as the input for our new ion evolution model.

In the previous paragraphs we discussed the additional production rate of small ions due to the waterfall. What is the character of these small ions? According to the mechanism proposed by Laakso *et al.* (2006), primary negative ions associated with a waterfall should be quite small. Examples of such ions are $OH^-(H_2O)_n$, where the number of water molecules (n) does not exceed ten and should rather equal three or four (Botti *et al.* 2004, Nagato *et al.* 2006). The mechanism proposed by Laakso *et al.* (2006) fails to take into account chemical impurities in water. A river water may contain large amounts of such impurities.

There is only a limited knowledge on how chemical additives can interfere with the mechanisms generating ions from droplets. Some authors have stated that the outer layers of a water solution droplet consist only of water molecules. Because of the versatility of hydrogen bonds, water can form shells around any impurities (Finney 2004, Petersen and Saykally 2005), so the outer shells should consist of water. According to the mechanism proposed by us, the produced negative ions originate mainly from the droplet surface. Therefore, our model fits with this assumption. However, several authors have shown that the outer shell does not consist solely of water molecules, in addition to which water molecules tend to be removed from the outer shell. Garret (2004) simulated water solutions containing NaF, NaCl, NaBr and NaI, showing that I^- and Br^- ions tend to be located at the surface whereas the other ions do not (e.g., more abundant natural Cl^- ions). Ellison *et al.* (1999) proposed 200 nm (sea) drops consisting of an aqueous core that is encapsulated in a hydrophobic organic layer. Znamenskiy *et al.* (2003) did not support the concept of a hydrophobic outer layer. The simulations of 6 nm water solution drops showed (1) that one can hardly speak about any geometrical outer shell because there are continuous surface fluctuations having an amplitude of as high as 1 nm, and (2) that hydrophobic ions tend to escape from the surface. The problem how ions are caught up from (inside) the droplets is highly important for the electrospray ionisation technique. However, the results describing the ESI effect can not directly be applied to the waterfall effect. This is because the ESI uses highly charged droplets, strong electric fields and solutions in which water is a minor constituent (Kebarle and Peschke 2000, Cech and Enke 2001). None of these factors can be found at a waterfall. Still, the above mentioned studies prove that several chemical compounds are likely to be at the surfaces of drops after the evaporation of water.

Since we need to have concrete ion species in our ion evolution scheme, we prefer the mechanism having $OH^-(H_2O)_n$ ions as the primary negative ions produced by the waterfall, despite the fact this mechanism cannot handle impurities in water. There are a few more arguments in favour of our mechanism. First, the "waterfall effect" also holds for distilled water (Lenard 1892, Chapman 1937, Iribarne and Thomson 1976), so our mechanism should be able to handle this "pure" case. Second, when the solution contains less than few milligrams of salt, the ion spectra are nearly the same as they are in case of distilled water (Chapman 1937, Iribarne and Thomson 1976). This suggests that our mechanism is able to handle dilute solutions. Third, some investigators have mentioned the OH^- ions in the context of the "waterfall effect", still not providing any further approaches (Chapman 1938).

There are some qualitative considerations that were not included in our simulations. The new $OH^-(H_2O)_n$ ions might catch neutral water clusters abundant near waterfalls. Water itself tends to form "magic" clusters $(H_2O)_n$ (n = 5, 10, 20, …, 280, …, etc.) that are more stable than other water clusters (Chaplin 2000, Ludwig 2001). The small negative ions catch readily water molecules, and entire "magic" water clusters can join with an ion. The new complexes can be quite large (e.g., the "magic" $(H_2O)_{280}$), and such complexes can be located within the intermediate ion region. Therefore, at least a fraction of abundant negative intermediate ions (Fig. 3) can consist of pure water, charged by OH^- ions.

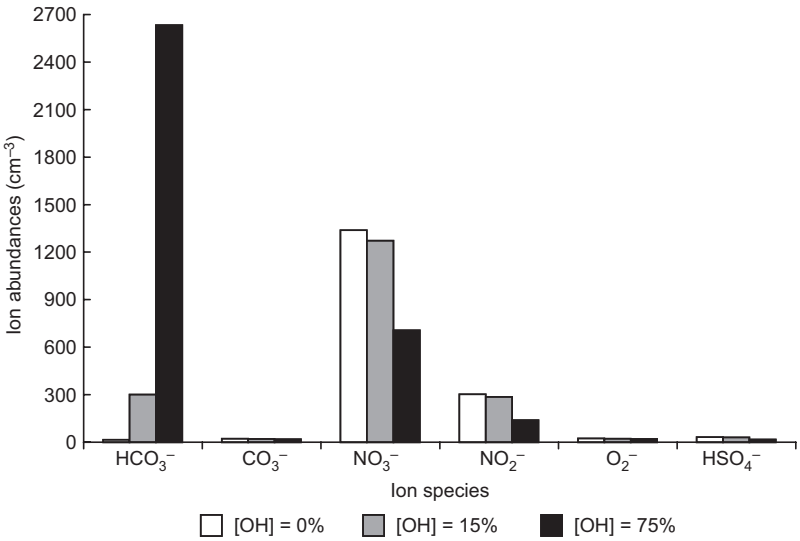

Fig. 5. Abundances of six steady-state ion families for case A1.

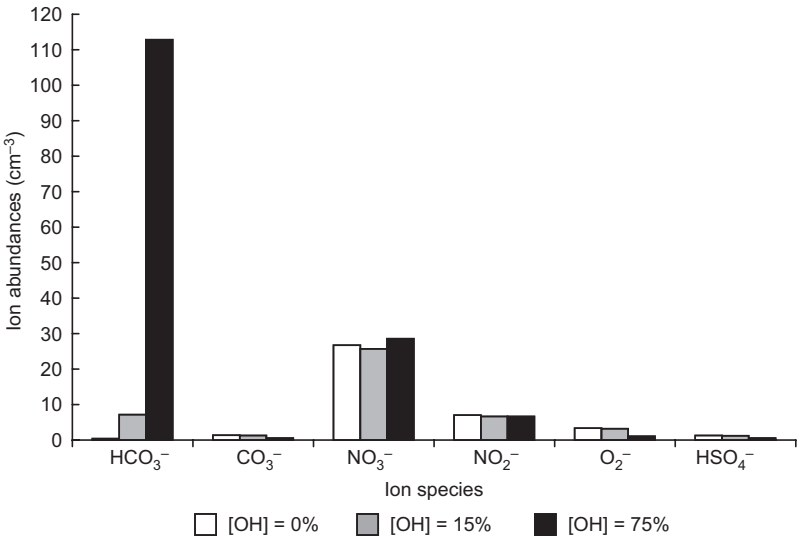

Fig. 6. Abundances of six steady-state ion families for case A2.

Simulation results

The simulation results are presented in Figs. 5–8 which show the steady-state ion composition for six ion families: $HCO_3^-()$, $CO_3^-()$, $NO_3^-()()$, $NO_2^-()$, $O_2^-()$ and $HSO_4^-()()$. Each ion family (class) can contain several ion species, but all the species in the same ion family contain the same core. Several molecules can surround the ion core. For example, the ion core NO_3^- in class $NO_3^-()()$ can be surrounded by HNO_3 and/or H_2O molecules. Chemical reactions within the classes (families) are much faster than those between the classes. For example, the reactions in classes $O_2^-()$ and/or $NO_3^-()$ proceed within microseconds, whereas the reactions transforming ion species in class $O_2^-()$ to those in class $NO_3^-()$ may take seconds. Therefore, a family can be regarded as a chain in its equilibrium state, whereas each of the families is chemically clearly distinct from another. In fact, this difference in reaction rates can be employed as a base for the definition of a class: all the species that are connected via reactions faster than a certain reference reaction rate can be regarded as a class. Partly, such a treatment is derived from the

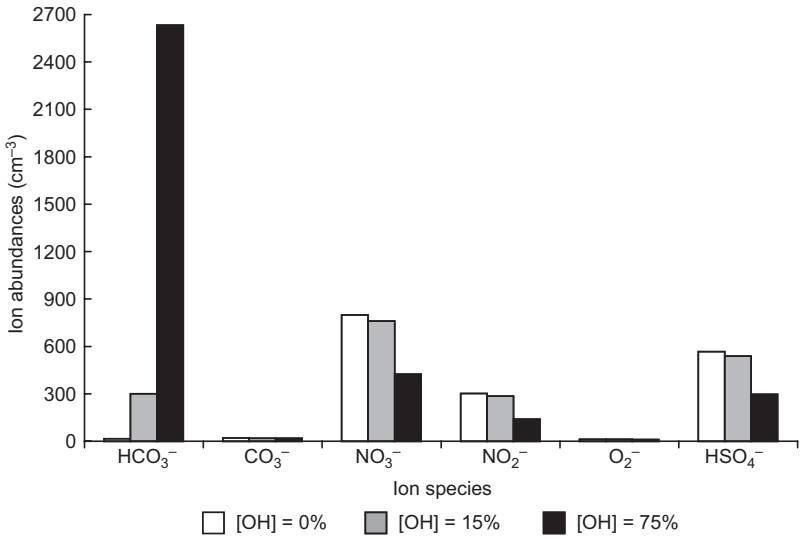

Fig. 7. Abundances of six steady-state ion families for case B1.

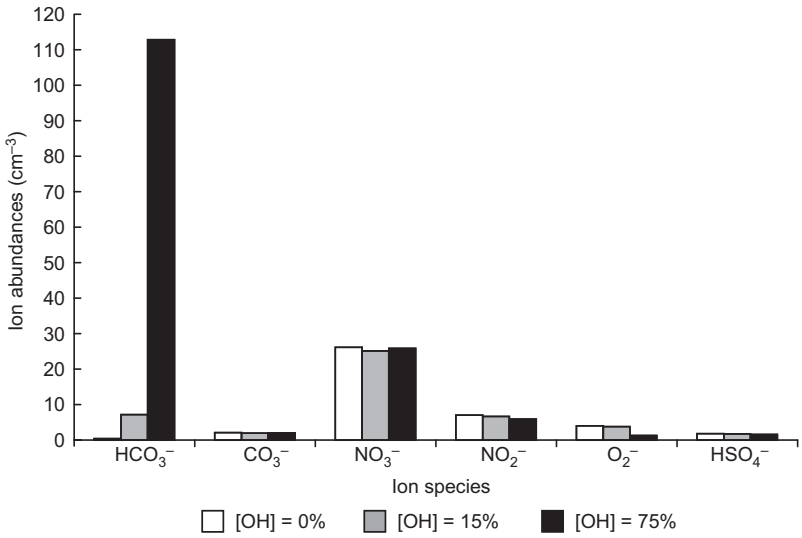

Fig. 8. Abundances of six steady-state ion families for case B2.

experimental fact that these families often appear as a whole. For example, by means of mobility spectrometry one can obtain distinct spectra of classes but no distinct spectra of individual species within classes. This standpoint was already introduced by Mohnen (1977).

The measurement results (Fig. 2) demonstrated that the waterfall generated negative small ions (diameter < 1.5 nm). We used this outcome in the ion evolution model. The new initial OH^- ions near the waterfall transmute the common evolution path. We simulated three different cases. In the first case the fraction of new OH^- ions was set to 0%, such that the initial ion mixture consisted only of O_2^- and O^- ions generated by ionising radiation in the atmosphere. This case corresponds to a situation far from the waterfall. In the second case 85% of the initial ion mixture consisted of O_2^- and O^- ions, exactly as it was in the first case (natural ionising radiation does not change), whereas 15% of the ions were OH^- ions supposed to have originated from the waterfall. In the third case only 25% of the initial ion mixture consists of O_2^- and O^- ions, with the rest 75% being OH^- ions from the waterfall. In the second and third (waterfall-induced)

cases the total concentration of all initial ions was higher than that in the first (natural) case.

Throughout all the simulations, the background ion production rate was assumed to be 5 cm^{-3} s^{-1}, as mentioned earlier, and the waterfall produced additional OH^- ions. As a result, the total ion production rate was equal to 5.9 cm^{-3} s^{-1} (5 cm^{-3} s^{-1} of common O_2^- and O^- ions, and 0.9 cm^{-3} s^{-1} of OH^- ions) in the second case and 20 cm^{-3} s^{-1} (5 cm^{-3} s^{-1} of common ions and 15 cm^{-3} s^{-1} of OH^- ions) in the third case.

We also varied the abundance of sulphuric acid and background aerosol particles. In cases A (Figs. 5–6) the concentration of sulphuric acid was set to 10^6 molecules cm^{-3}, and in cases B (Figs. 7–8) it was 10^8 molecules cm^{-3}. In cases A1 and B1 (Figs. 5 and 7) the concentration of background aerosol particles was set to 100 particles cm^{-3}, whereas in cases A2 and B2 (Figs. 6 and 8) it was 100 000 particles cm^{-3}. Because of variations in the background aerosol particle concentration, and because of the additional primary OH^- ions, the total steady-state concentration of all ions changed as well. We therefore varied the concentration scales between Figs. 5–8. As one might expect, higher aerosol particle concentrations resulted in lower ion concentrations, whereas additional OH^- primary ions resulted in higher total ion concentrations.

The results can be attributed to four specific environmental cases A1, A2, B1 and B2. All these cases can be considered somewhat hypothetical because such environmental situations are quite rare, and case B2 (Fig. 8) is the most hypothetical one. Commonly, the daytime concentration of sulphuric acid is in the range 10^6–10^8 cm^{-3}, and the number concentration of aerosol particles is in the range 10^2–10^5 cm^{-3}. Therefore, these four cases can be regarded as the corners of the daytime proper feature space of ion spectra. Since we do not know the exact initial values of concentrations, our choice to present the limits of the proper feature space should be a reasonable one. The cases characterized by high number concentrations of aerosol particles showed very low ion concentrations (Figs. 6 and 8). Even when the waterfall produced small ions at a maximum rate, the total small ion concentration remained below 200 cm^{-3}. Natural situations are expected to be well inside the corners of this feature space. We also simulate a situation in which the H_2SO_4 concentration was below 10^6 cm^{-3} in order to find out what would take place during the night-time. In this case, the result did not differ more than 5% from those obtained using the H_2SO_4 concentration of 10^6 cm^{-3} (Figs. 5–6), except that the model predicted almost no HSO_4^- core ions.

The most prominent simulation outcome was the dominance of a new ion family: HCO_3^- core ions. Along with an increase in the abundance of new OH^- initial ions, which we presume to exist due to waterfall processes, the percentage of this new ion family increased. Variations in sulphuric acid or background aerosol particle concentrations did not disturb this effect. If the fraction of initial OH^- ions was 75%, the new HCO_3^- core ions were dominant in all the cases. Near the waterfall, NO_3^- and HSO_4^- core ions were found to be suppressed, whereas HCO_3^- core ions were found to become dominant ones. The presence of sulphuric acid did not change this "waterfall effect": if OH^- ions were initially abundant (such as near the waterfall), all the other ion families were decreased in abundance, even at very high concentration levels of sulphuric acid (Figs. 7 and 8).

Our simulation showed that waterfall-induced OH^- ions result in steady-state HCO_3^- core ions despite the many new competitive reaction routes. We further showed that this process takes place not only within a millisecond scale (*see* Huertas *et al*. 1978), but is also relevant to natural situations.

Conclusions

According to our previous measurements, waterfalls permanently modify air ion spectra. In this paper we investigated the possible chemical nature of the air ions arising from near waterfalls.

We assumed that the waterfall enhances the concentration of OH^- ions. This assumption is supported by published studies and by relevant chemical considerations. Water itself can produce negative OH^- cluster ions, which alters the ion evolution scheme. According to our simulations, a new HCO_3^-•X•Y family dominates,

while all other ion families are suppressed. Far from the waterfall, the main small air ion clusters are the NO_3^-•X•Y and/or HSO_4^-•X•Y ion families.

We demonstrated that many results that have formerly been found to dominate within a millisecond scale are also valid at natural situations. We further put the results into the context of the "waterfall effect".

Our measurements also showed an enhanced concentration of intermediate (diameters from 1.5 to 10 nm) negative ions near the waterfall, compared with the reference point far from the waterfall. We suggest that these intermediate ions can, to a large extent, consist of a OH^- core and "magic" water clusters.

Acknowledgements: This research has been supported by the Estonian Science Foundation grants 6223 and 6988 and by the University of Tartu research project PP1FY07913.

References

Blanchard D. 1958. Electrically charged drops from bubbles in seawater and their meteorological significance. *Journal of Meteorology* 15: 383–395.

Botti A., Bruni F., Imberti S., Ricci M.A. & Soper A.K. 2004. Solvation shell of OH^- ions in water. *J. Mol. Liquids* 117: 81–84.

Brown T.L., LeMay H.E., Bursten B.E. & Murphy C.J. 2006. *Chemistry: the central science*, Pearson Education, NY.

Cech N. & Enke C. 2001. Practical implications of some recent studies in electrospray ionisation fundamentals. *Mass Spectrom. Rev.* 20: 362–387.

Chaplin M.F. 2000. A proposal for the structuring of water. *Biophys. Chem.* 83: 211–221.

Chapman S. 1937. Carrier mobility spectra of spray electrified liquids. *Phys. Rev.* 52: 184–190.

Chapman S. 1938. Interpretation of carrier mobility spectra of liquids electrified by bubbling and spraying. *Phys. Rev.* 54: 528–533.

Ellison G.B., Tuck A.F. & Vaida V. 1999. Atmospheric processing of organic aerosols. *J. Geophys. Res.* 104: 11633–11641.

Finney J. 2004. Water? What's so special about it? *Phil. Trans. R. Soc. Lond. B* 359: 1145–1165.

Garrett B.C. 2004. Ions at the air/water interface. *Science* 303: 1146–1147.

Gathman S. & Trent E.M. 1968. Space charge over the open ocean. *J. Atmos. Sci.* 25: 1075–1079.

Han B., Lenggoro I.W., Choi M. & Okuyama K. 2003. Measurements of cluster ions and residue nanoparticles from water samples with an electrospray/differential mobility analyzer. *Analytical Sciences* 19: 843–851.

Hirsikko A., Laakso L., Hõrrak U., Aalto P., Kerminen V.-M. & Kulmala M. 2005. Annual and size dependent variation of growth rates and ion concentrations in boreal forest. *Boreal Env. Res.* 10: 357–369.

Huertas M.L., Fontan J. & Gonzalez J. 1978. Evolution times of tropospheric negative ions. *Atmos. Environ.* 12: 2351–2362.

Iribarne J.V. & Thomson B.A. 1976. On the evaporation of small ions from charged droplets. *J. Chem. Phys.* 64: 2287–2294.

Kebarle P. & Peschke M. 2000. On the mechanisms by which the charged droplets produced by electrospray lead to gas phase ions. *Analytica Chimica Acta* 406: 11–35.

Klusek Z., Wiszniewski A. & Jakacki J. 2004. Relationships between atmospheric positive electric charge densities and gas bubble concentrations at Baltic Sea. *Oceanologia* 46: 459–476.

Laakso L., Petäjä T., Lehtinen K.E.J., Kulmala M., Paatero J., Hõrrak U., Tammet H. & Joutensaari J. 2004. Ion production rate in a boreal forest based on ion, particle and radiation measurements. *Atmos. Chem. Phys.* 4: 1933–1943.

Laakso L., Hirsikko A., Grönholm T., Kulmala M., Luts A. & Parts T. 2006. Waterfall as a source of small charged aerosol particles. *Atmos. Chem. Phys. Discuss.* 6: 9297–9314.

Lenard P. 1892. Über die Elektrizität der Wasserfälle. *Ann. Phys. Lpz.* 46: 584–636.

Ludwig R. 2001. Water: from clusters to the bulk. *Angew. Chem. Int. Ed.* 40: 1808–1927.

Luts A. 1998. Temperature variation of the evolution of positive small air ions at contant relative humidity. *Journal of Atmospheric and Solar-Terrestrial Physics* 60: 1739–1750.

Luts A. & Parts T. 2002. Evolution of negative small air ions at two different temperatures. *Journal of Atmospheric and Solar-Terrestrial Physics* 64: 763–774.

Luts A., Noppel M. & Vehkamäki H. 2004. Effect of sulfuric acid on the composition of negative small air ions: a numerical simulation. *J. Aerosol Sci.* 35, Suppl. 2: S953–S954.

Mirme A., Tamm E., Mordas G., Vana M., Uin J., Mirme S., Bernotas T., Laakso L., Hirsikko A. & Kulmala M. 2007: A wide-range multi-channel Air Ion Spectrometer. *Boreal Env. Res.* 12: 247–264.

Mohnen V.A. 1977. Formation, nature and mobility of ions of atmospheric importance. In: Dolezalek H. & Reiter R. (eds.), *Electrical processes in atmospheres,* D. Steinkopff Verlag, Darmstadt, pp. 1–17.

Nagato K., Matsui Y., Miyata T. & Yamauchi T. 2006. An analysis of the evolution of negative ions produced by a corona ionizer in air. *Int. J. Mass Spectrom.* 248: 142–147.

Petersen P.B. & Saykally R.J. 2005. Evidence for an enhanced hydronium concentration at the liquid water surface. *J. Phys. Chem. B* 109: 7976–7980.

Reiter R. 1994. Charges on particles of different size from bubbles of Mediterranean Sea surf and from waterfalls. *J. Geophys. Res.* 99: 10807–10812.

Salm J. [Сальм Й.] 1987. [Combination of air ions in the

case of symmetrical steady-state ionization]. *Acta et commentationes Universitatis Tartuensis* 755: 10–17. [In Russian].

Sennikov P.G., Ignatov S.K. & Schrems O. 2005. Complexes and clusters of water relevant to atmospheric chemistry: H_2O complexes with oxidants. *ChemPhysChem* 6: 392–412, doi: 10.1002/cphc.200400405.

Shin J.-W., Hammer N.I., Diken E.G., Johnson M.A., Walters R.S., Jaeger T.D., Duncan M.A., Christie R.A. & Jordan K.D. 2004. Infrared signature of structures associated with the $H^+(H_2O)_n$ (n = 6 to 27) clusters. *Science* 304: 1137–1140.

Seinfeld J.H. & Pandis S.N. 1998. *Atmospheric chemistry and physics*, John Wiley & Sons Inc., New York.

Tammet H. 1995. Size and mobility of nanometer particles, clusters and ions. *J. Aerosol Sci*. 26: 459–475.

Tammet H. & Kulmala M. 2005. Simulation tool for atmospheric aerosol nucleation bursts. *J. Aerosol Sci*. 36: 173–196.

Vostrikov A.A., Drozdov S.V., Rudnev V.S. & Kurkina L.I. 2006. Molecular dynamics study of neutral and charged water clusters. *Computational Materials Science* 35: 254–260.

Znamenskiy V., Marginean I. & Vertes A. 2003. Solvated ion evaporation from charged water nanodroplets. *J. Phys. Chem. A* 107: 7406–7412.

Zwier T.S. 2004. The structure of protonated water clusters. *Science* 304: 1119–1120.